Marine and Petroleum Geology xxx (2014) 1–9

Contents lists available at ScienceDirect

Marine and Petroleum Geology

journal homepage: www.elsevier.com/locate/marpetgeo

Research paper

# Sampling disturbance in hydrate-bearing sediment pressure cores: NGHP-01 expedition, Krishna–Godavari Basin example

Sheng Dai [a, *], J. Carlos Santamarina [b]

[a] National Energy Technology Laboratory, U.S. Department of Energy, 3610 Collins Ferry Road, Morgantown, WV 26507, USA
[b] Georgia Institute of Technology, 790 Atlantic Dr., Atlanta, GA 30332, USA

ARTICLE INFO

*Article history:*
Received 10 February 2014
Received in revised form
11 July 2014
Accepted 15 July 2014
Available online xxx

*Keywords:*
Sampling effect
Pressure core
Mandel–Cryer effect
Fine sediment
Anomalous preservation

ABSTRACT

Sampling natural sediments causes unavoidable disturbance as recovered sediments experience changes in stress and strain during drilling, core recovery, transportation, handling, and early stages of testing. In hydrate-bearing sediments, the potential for sampling disturbance may be aggravated, since pressure and temperature changes can lead to hydrate dissociation and gas exsolution. Pressure core technology attempts to recover and characterize hydrate-bearing sediments while preserving them under in situ pressure and temperature conditions, which is an essential requirement to assess the mechanical, physical, chemical, and biological properties of natural hydrate-bearing sediments. Previous studies on near-surface sampling effects are extended in this study to evaluate additional sampling disturbances relevant to hydrate-bearing sediments: (1) hydrate dissociation due to mechanical extension, (2) negative pore pressure generation during unloading (Mandel–Cryer effect), (3) secondary hydrate formation, (4) changes in hydrate mass as a function of changes in pressure and temperature within the stability field, (5) hydrate anomalous preservation and its benefits for pressure core handling and testing, and (6) relaxation/aging following sampling. Results provide valuable insight to sampler design, coring and operation procedures, high pressure chamber design, and pressure core testing techniques.



## 1. Introduction

The 2006 Indian National Gas Hydrate Program (NGHP) Expedition 01 was conducted to investigate geological and geochemical controls on gas hydrate occurrence offshore of the Indian Peninsula and along the Andaman convergent margin (Collett et al., 2006). Hydrate saturation estimated from compressional wave velocity, electrical resistivity logs, and X-ray computed tomography vary from $S_h < 5\%$ to as high as $S_h = \sim 80\%$ (Lee and Collett, 2009; Shankar and Riedel, 2011).

The eastern continental margin of India formed as the result of rifting between India and the rest of East Gondwanaland (Australia/Antarctica) in the Late Jurassic and Early Cretaceous. Plate reconstructions place the eastern Indian margin adjacent to Enderby Land in East Antarctica with the northern margin of "Greater India" along the western margin of Australia (Bastia and Nayak, 2006; Krishna et al., 2000). The Krishna–Godavari Basin came into existence following rifting along eastern continental margin of Indian Craton in the early Mesozoic. The Krishna–Godavari Basin contains about 5 km of sediments with several depositional sequences, ranging in age from Late Carboniferous to Pleistocene (Bastia and Nayak, 2006). Sediment input to the Bay of Bengal is dominated by the Ganges–Brahmaputra River system, resulting in the development of the Bengal Fan. Isopach maps show 8–10 km of sediment at the location of the NGHP-01 drill sites established in the Krishna–Godavari Basin. The sedimentary section in the Krishna–Godavari Basin is dominated by clay-rich sediments, with little evidence of significant input of coarser-grain sediments (Basu, 1990). Studies of conventional hydrocarbon systems in the Krishna–Godavari Basin have revealed that preserved organic matter in Paleocene and Cretaceous sedimentary section has led to the accumulation of significant conventional gas and gas-condensate fields in the basin (Banerjie et al., 1994). However, the gas hydrates sampled during NGHP-01 contain mostly methane derived from microbial sources (Collett et al., 2008).

For the most part, gas hydrate formation in the Krishna–Godavari Basin has developed by grain-displacement processes and has yielded gas hydrate in the form of nodules, veins, and lenses (Rees et al., 2011); this hydrate morphology is inherently caused by high capillary forces associated with the hydrate–water

* Corresponding author.
*E-mail addresses:* dais@netl.doe.gov (S. Dai), jcs@gatech.edu (J.C. Santamarina).

http://dx.doi.org/10.1016/j.marpetgeo.2014.07.013
0264-8172/

interface in fine-grained sediments (Clennell et al., 1999; Dai et al., 2012; Henry et al., 1999). Capillary pressure effects in these sediments also constrain the thickness of the hydrate stability zone at the sites in the Krishna–Godavari Basin. The equilibrium gas hydrate temperature depression $\Delta T_{dep}$ in a cylindrical pore space can be estimated as (Kwon et al., 2008):

$$\Delta T_{dep} = -\frac{2}{d_{pore}}\left(\frac{\gamma_{hw} m_h \cos\theta}{\rho_h L_f}\right) T_{bulk} \quad (1)$$

where $\gamma_{hw}$ and $\theta$ are the surface tension and contact angle between hydrate and water, $m_h$ and $\rho_h$ are the molecular weight and density of hydrate, $L_f$ is the latent heat of hydrate dissociation, and $T_{bulk}$ is the equilibrium temperature in unconfined bulk solution. The pore size $d_{pore}$ depends on sediment void ratio $e$, specific surface $S_s$, and mineral mass density $\rho_m$ as: $d_{pore} = 2e/(\rho_m S_s)$, and the void ratio $e$ changes with depth as $e = e_{100} + C_c \log(\sigma'/\text{kPa})$, where $e_{100}$ and $C_c$ are sediment-dependent parameters (Burland, 1990). Figure 1 shows the altered hydrate stability boundaries that could be anticipated in the Krishna–Godavari Basin for three common clay minerals identified in the basin, each with distinct specific surface and compressibility: kaolinite, illite, and montmorillonite. In agreement with predictions in Figure 1, reported depths to the base of the hydrate stability zone in clay- to silt-rich sediments can vary between 100 m and 200 m from expected conditions in coarser-grain sand-rich systems (Collett et al., 2008). Contrary to coarse sediments, such as those encountered in Alaska permafrost settings (Dai et al., 2011), pore size as it relates to the presence of fine-grained sediments at Krishna–Godavari can restrict the thickness of the hydrate stability zone.

Both conventional and pressure cores were recovered during the 2006 NGHP-01 expedition. Five pressure cores recovered at Site NGHP-01-21 were kept at 4 °C and 13 MPa fluid pressure, and tested three months after the expedition at an onshore facility in Singapore using the Instrumented Pressure Testing Chamber (IPTC) (Yun et al., 2010). The test program included the measurement of elastic wave velocities, shear strengths, electrical conductivities, and monitored fast depressurization tests using sub-sampled core samples. X-ray images showed horizontal layering, pronounced heterogeneity from milli- to centimeter scales, with the presence of high-density nodules and both horizontal and sub-vertical gas hydrate lenses. However, the laboratory testing of all natural sediments faces inherent sampling disturbance (Hvorslev, 1949), which occur even before detailed laboratory characterizations. This manuscript reviews previous studies on sampling effects associated with near surface sediment coring and processing, demonstrates the need for pressure core technology in the study of hydrate-bearing sediments, and analyzes several emergent phenomena of the poroelastic and pressure/temperature effects on hydrate-bearing sediment cores.

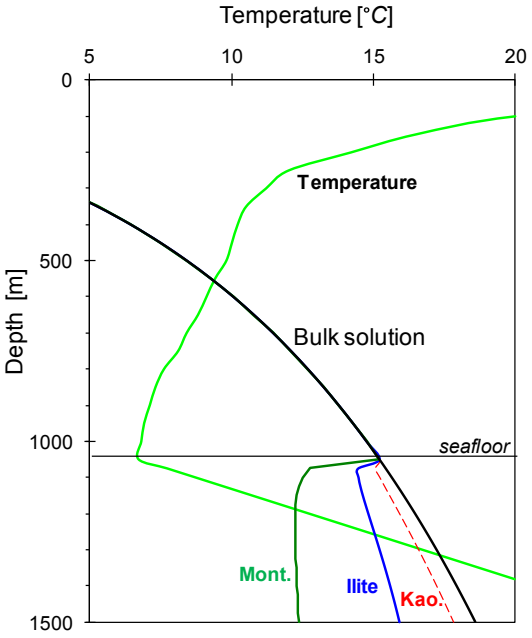


**Figure 1.** Pore size dependent shift in the phase boundary at Krishna–Godavari Basin site. Trends are computed for bulk solution, kaolin "Kao" ($e_{100} = 0.89$, $C_c = 0.29$), illite ($e_{100} = 2.05$, $C_c = 0.82$), and Montmorillonite "Mont." ($e_{100} = 3.06$, $C_c = 1.15$).

## 2. Sampling disturbance in hydrate-free sediment cores

Sampling affects the mechanical, biological, chemical, mineralogical, and lithological properties of natural sediments. Cores experience excavation unloading and friction against the corer wall, introducing unavoidable volumetric and shear strains. Figure 2 illustrates a conceptual stress-strain path that a sediment experiences during coring (Hight et al., 1992; La Rochelle et al., 1980; Ladd and DeGroot, 2003; Landon, 2007; Shogaki and Kaneko, 1994). To rationally quantify sampling disturbances, the "perfect sampling approach" considers only the unavoidable undrained removal of the deviator stress ($q \rightarrow 0$), followed by an undrained triaxial extension; and the "ideal sampling approach" considers also the effects of sequentially compression and extension along the centerline, shear strain along sampling tube walls during sampler penetration, and undrained shear stress relief during sample extrusion (Baligh, 1985; Baligh et al., 1987; Levadoux and Baligh, 1980).

### 2.1. Sources of sampling disturbance

Several factors account for changes in physical and mechanical properties of sampled sediments. These factors include, (1) Drilling and coring has been shown to cause changes in effective stress and

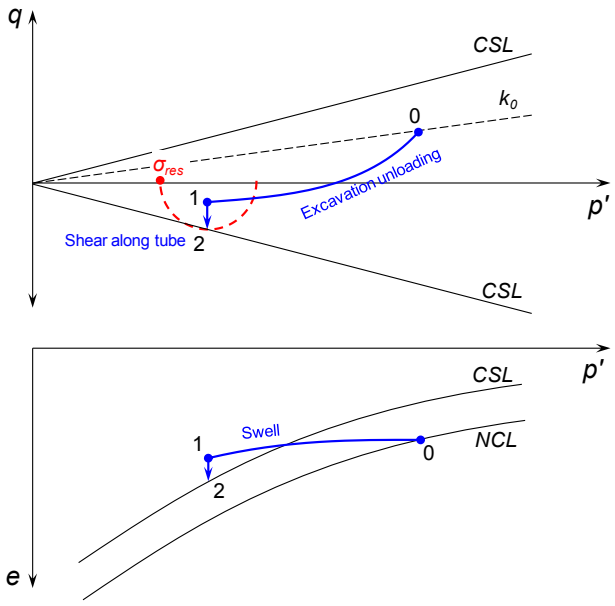


**Figure 2.** The stress-strain path during sampling. Cores experience excavation unloading (0 → 1) and wall shear (1 → 2); volumetric (shown) and shear strains are unavoidable (Note: CSL = critical state line; NCL = normal consolidation line; $\sigma_{res}$ = residual stress mobilized during expansion against the sampling tube).

Please cite this article in press as: Dai, S., Santamarina, J.C., Sampling disturbance in hydrate-bearing sediment pressure cores: NGHP-01 expedition, Krishna–Godavari Basin example, Marine and Petroleum Geology (2014), http://dx.doi.org/10.1016/j.marpetgeo.2014.07.013

fluid pressure, which leads to associated strain (Baligh et al., 1987; Cao et al., 2007; Clayton et al., 1998; Li et al., 1997). It has also been shown that the stress caused by the high drilling mud pressures required to circulate the slurry and remove drill cuttings from the well can be more detrimental than the unloading stress induced by drilling and corer penetration (Chung et al., 2004). (2) Sampling related effects on the core can include effective stress relaxation (Chau, 1991; La Rochelle et al., 1980), friction along the sampling tube or wall shear (Baligh et al., 1987; Chau, 1991; Clayton and Siddique, 1999), deformation due to insufficient rigidity of the sampling tube, and pore pressure variation (Clayton and Siddique, 1999; Safaqah and Riemer, 2006; Siddique et al., 1999). (3) It has also been shown that core storage and transportation of the specimen can result in temperature variation, sampler deformation, vibrations, and drying of the core (Baligh et al., 1987; Shogaki and Kaneko, 1994). (4) Core handling and testing can also impose additional disturbance associated with sample extrusion (Baligh et al., 1987; Chung et al., 2004; Day, 1990), specimen trimming to the required lab equipment dimensions (Atkinson et al., 1992; Baligh et al., 1987), and specimen installation in test chambers (Hight et al., 1992).

### 2.2. Core disturbance evaluation and assessment

Visual inspection (Hvorslev, 1949; Long, 2003) and X-ray radiography (ASTM D4452) provide direct "geometric" evidence of disturbance. Numerous studies have been conducted to measure physical/mechanical changes due to sampling. Observations include: (1) decrease in undrained shear strength $s_u$ and preconsolidation stress $p_c$ particularly in soils with low plasticity (Baligh et al., 1987; Long, 2003; Tanaka et al., 2001; Zhang and Lunne, 2002); (2) increase in volumetric strain $\varepsilon_v$, axial strain $\varepsilon_a$,

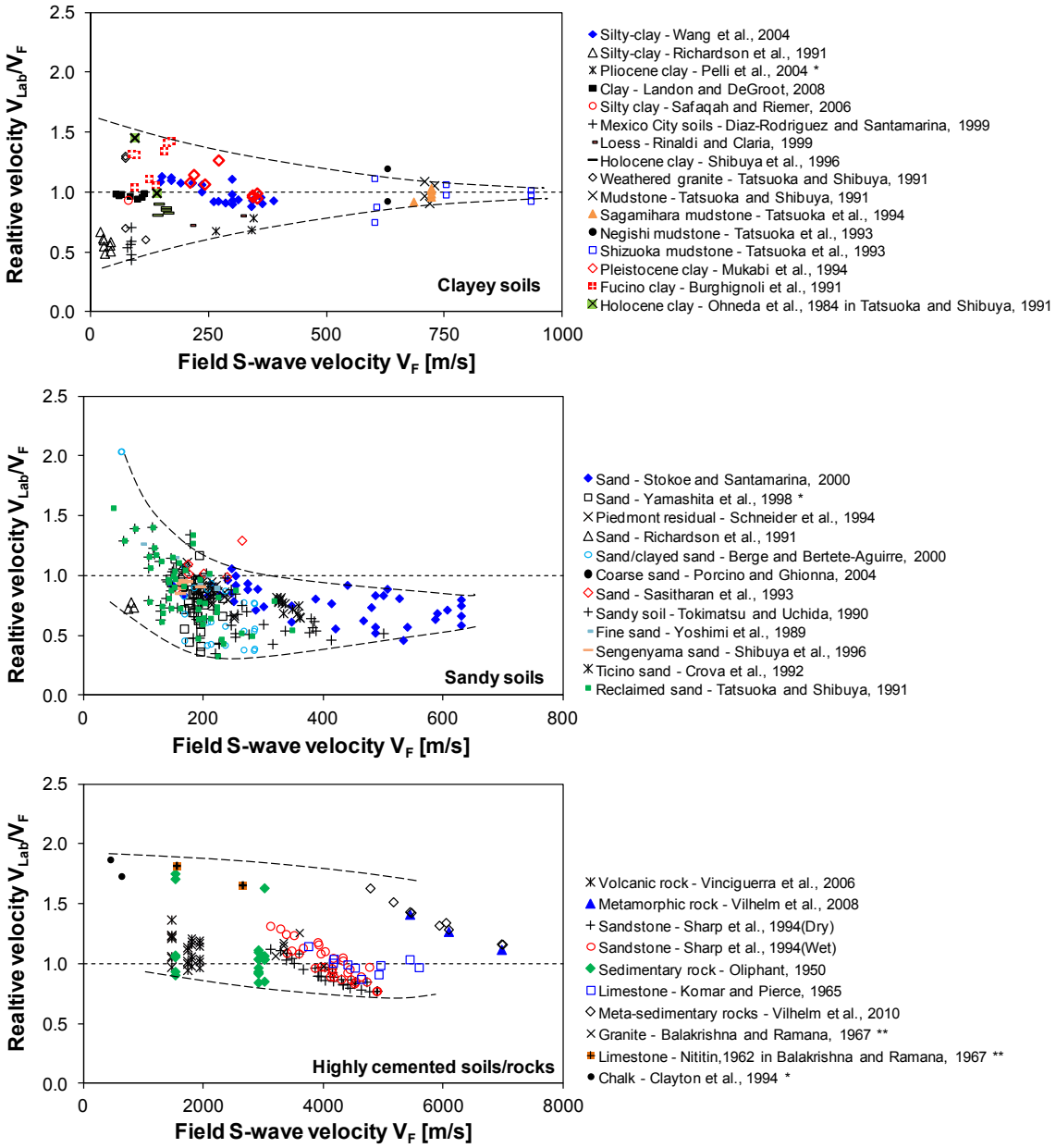


**Figure 3.** Sampling disturbance and sediment type. Note: * values computed from $G_{max}$ assuming specimen density $\rho = 2000$ kg/m$^3$; ** Computed from $V_p$ measured in unsaturated specimens assuming $V_p/V_s = 1.5$.

Please cite this article in press as: Dai, S., Santamarina, J.C., Sampling disturbance in hydrate-bearing sediment pressure cores: NGHP-01 expedition, Krishna–Godavari Basin example, Marine and Petroleum Geology (2014), http://dx.doi.org/10.1016/j.marpetgeo.2014.07.013

and shear strain $\varepsilon_s$ at peak deviatoric stress (Giao et al., 2004; Hird and Hajj, 1995; Santagata and Germaine, 2005); smaller sampling strains in over-consolidated clays (Siddique et al., 1999); (3) decrease in most consolidation parameters in normally consolidated soils, such as compression index $C_c$, coefficient of volume compressibility $m_v$, and coefficient of consolidation $c_v$ (Shogaki and Kaneko, 1994); and (4) pore pressure variation during coring, specimen extrusion, and specimen trimming (Kimura and Saitoh, 1984; Safaqah and Riemer, 2006).

The change in shear stiffness (S-wave velocity) from values measured in situ $V_F$ to those measured in the laboratory $V_{lab}$ at the same stress conditions is a good indicator of disturbance (Landon et al., 2007). The extent of sampling disturbance also depends on soil type (Rinaldi and Santamarina, 2008; Stokoe and Santamarina, 2000; Tatsuoka and Shibuya, 1991). Figure 3 shows shear wave velocities of clays, sands, and cemented soils/rocks obtained both in the field $V_F$ and the laboratory $V_{Lab}$. It has been observed that (1) soft clayey or fine-grained sediments can either gain (reconsolidation upon reloading to in situ effective stress conditions) or lose stiffness during sampling (destructuring caused by coring induced strains); (2) stiff clayey sediments tend to experience smaller sampling induced stiffness changes, suggesting that the fabric of stiff clayey soils can be well preserved; (3) loose sandy coarse-grained soils tend to gain stiffness due to densification; (4) most coarse-grained soils tend to lose stiffness during sampling due to dilation and/or the loss of diagenetic cementation during sampling. Softening during sampling should be expected in most coarse-grained sediments with a field velocity $V_F > 150–200$ *m/s*; and (5) cemented soils or rocks ($V_s > 1000$ m/s) are also affected by sampling. But most importantly, sampling bias has the greatest effect on most measured parameters. For example, small laboratory specimens do not include joints and faults encountered in the field, hence $V_{lab}/V_F$ can be highly elevated, while microfracturing is responsible for the drop in $V_{lab}/V_F$ (Eberhardt et al., 1999).

## 3. Hydrate-bearing sediments: additional sampling effects

Accumulating experience with pressure core technology has demonstrated that sediments with various concentrations of gas hydrate can be recovered at near in situ pressure conditions. In many cases, sampling disturbances associated with hydrate-free sediments can also be applied to our understanding of hydrate-bearing sediment related core disturbance. However, additional effects are anticipated due to pressure and temperature dependency of hydrate dissolution and dissociation, and the pronounced time dependent relaxation of crystalline hydrate. These effects are explored next.

### 3.1. Pore-scale analysis

In situ hydrate-bearing sediments are subjected to effective stress, temperature, and water pressure conditions within the hydrate stability field. Figure 4 illustrates a pore-scale analysis of potential sampling effects. As shown, coring releases effective stress and induces matrix sediment skeleton expansion (Figure 4b). Tensile strain localization at cemented contacts causes bulk hydrate fracturing or debonding, and the potential for local hydrate dissociation even while the sample pressure and temperature conditions remain in the stability field (Jung and Santamarina, 2011). Methane hydrate within the stability zone may still dissociate during mechanical compaction tests, causing ductile deformation of hydrate crystals and free water release (Durham et al., 2003).

The insertion of the corer bit and barrel generates shear along the core (Figure 4c). Shear strains leads to dilation in dense-packing sediments or contraction in loose-packing sediments. Such volume changes (or associated pore pressure variation during rapid sampling) may alter hydrate cementation and stability.

Gas hydrate dissociates when depressurization takes the specimen outside the hydrate stability field (Figure 4d). Degassing is typically associated with volume expansion, fines migration, gas-driven fractures (Jung et al., 2011; Santamarina and Jang, 2009), and carbon isotope fractionation of $CH_4$ (Wallace et al., 2000). Hydrate dissociation leads to pore water freshening and the decrease in salt concentration that alters inter-particle electrical forces and surface properties of clay particles (Santamarina et al., 2001). The loss of hydrate mass decreases the sediment bulk stiffness; loss in shear stiffness will depend on pore habit and initial hydrate saturation (Lee et al., 2010). Additionally, depressurization

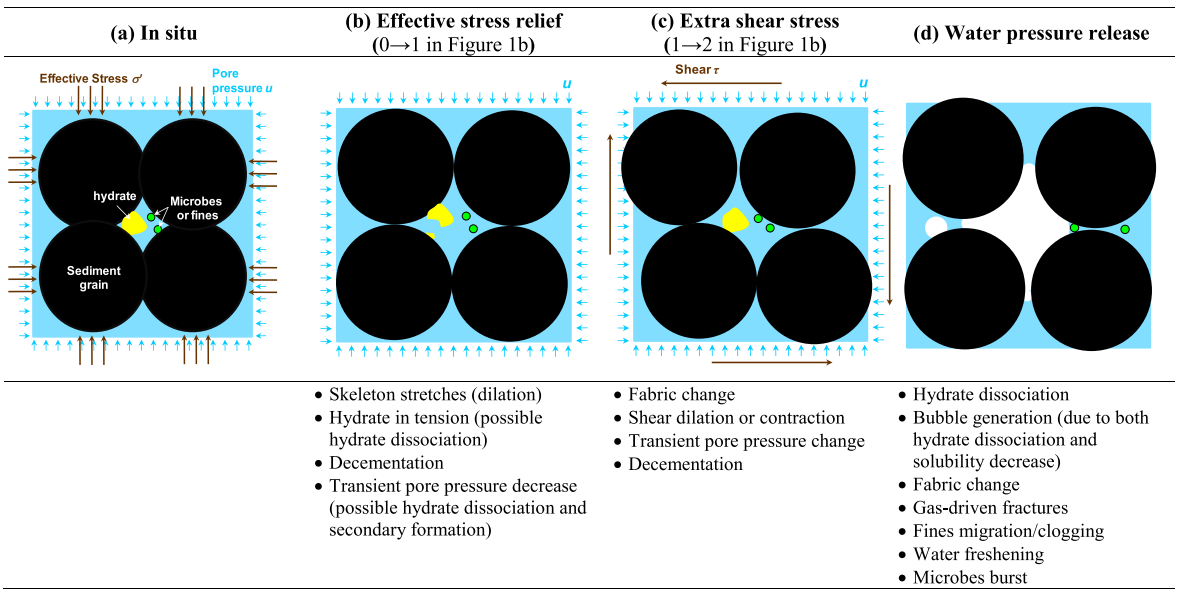


**Figure 4.** Sampling hydrate-bearing sediments. (a) In situ. (b, c) Unloading effective stress and induced shear in pressure cores. (d) The additional consequences of water pressure release in standard core.

Please cite this article in press as: Dai, S., Santamarina, J.C., Sampling disturbance in hydrate-bearing sediment pressure cores: NGHP-01 expedition, Krishna–Godavari Basin example, Marine and Petroleum Geology (2014), http://dx.doi.org/10.1016/j.marpetgeo.2014.07.013

can also negatively impact pressure sensitive microbial communities (Hemmingsen and Hemmingsen, 1980; Park and Clark, 2002).

All the above mentioned processes may preferentially affect the specimen outer edges due to core wall shear and the specimen center due to transient poroelastic effects as discussed next.

### 3.2. Unloading: poroelastic Mandel–Cryer effect and secondary hydrate formation

The pore pressure response to a sudden stress change is not homogenous throughout the specimen. This phenomenon is called the Mandel–Cryer effect (Cryer, 1963; Mandel, 1953). Unloading-induced skeleton rebound during sampling produces a drop in pore pressure particularly at the center of the specimen (Safaqah and Riemer, 2006).

The unloading $\Delta\sigma$ induced temporal and spatial variation of pore pressure $u$ (in the form of Laplace transform $\tilde{u}$) in a cylindrical soil specimen radius $R$ under zero lateral strain conditions is (Appendix A) :

$$\tilde{u} = M\left(1 - \frac{\alpha\eta}{GS}\right)A_1 I_0\left(r\sqrt{s/c}\right) - \alpha M A_2. \quad (2)$$

Numerical inversion of the Laplace transform of this equation returns the relative pore pressure decrease ($\Delta u/\Delta\sigma$) in terms of the dimensionless radius $\rho = x/R$, where $x$ is the distance from the center of the core. Results in Figure 5b are presented for different dimensionless time values $\tau = t/(R^2/c_v)$, where $c_v$ is the pore water pressure diffusion coefficient (refer to Table 1 for parameter values used in this computation). In this case, sediment permeability and compressibility determine the pore pressure diffusion coefficient $c_v$ in the dimensionless time $\tau$.

At the beginning of unloading, the skeleton rebound is hindered by the "stiff pore water", causing pore pressure decrease across the specimen ($\tau = 0$ in Fig. 5b). The pore pressure at boundaries immediately recovers, creating 'weakened' boundaries accompanied by a load transfer to inner zones. This leads to additional pore pressure drops $\Delta u > \Delta\sigma$ towards the center of the specimen ($\rho < 0.7$ and $\tau = 0.01$–$0.1$ in Fig. 5b). The maximum pore pressure drop occurs at the center of the specimen at time $\tau = t/(R^2/c_v) \approx 0.06$ and it exceeds the in situ vertical effective stress, $\Delta u = -1.17\Delta\sigma$ (Note: $\Delta u = -1.28\Delta\sigma$ for spherical geometry). The magnitude of maximum pore pressure drop increases with unloading rate, that is coring speed $v_{coring}$, since slower unloading allows more time for pore water pressure diffusion and homogenization (Fig. 5c).

Transient decrease in pore pressure can trigger hydrate dissociation, fluid expansion, and gas-driven opening-mode discontinuities across the cross section of the core. As the pore pressure recovers, secondary hydrate may form. This sampling effect should be expected when the in situ fluid pressure $u_o$ and effective stress $\sigma_o'$ are such that

$$u_o - 1.17\sigma_o' < u_{PB} \quad \text{where} \quad u_{PB} = f\left(T_{coring}\right) \quad (3)$$

where $u_{PB}$ is the fluid pressure at the hydrate phase boundary for the local temperature conditions during coring $T_{coring}$. In other words, Mandel–Cryer effects will manifest when the in situ fluid pressure is low, the effective stress is high and/or the temperature during coring is high.

Slices of the core X-ray tomogram obtained from hydrate-bearing sediments recovered from the Ulleung Basin are shown in Figure 6 for different rotations. The vertical hydrate lense aligned with the core main axis observed in the images clearly show this potential sampling effect (Fugro percussion Pressure Corer). Similar

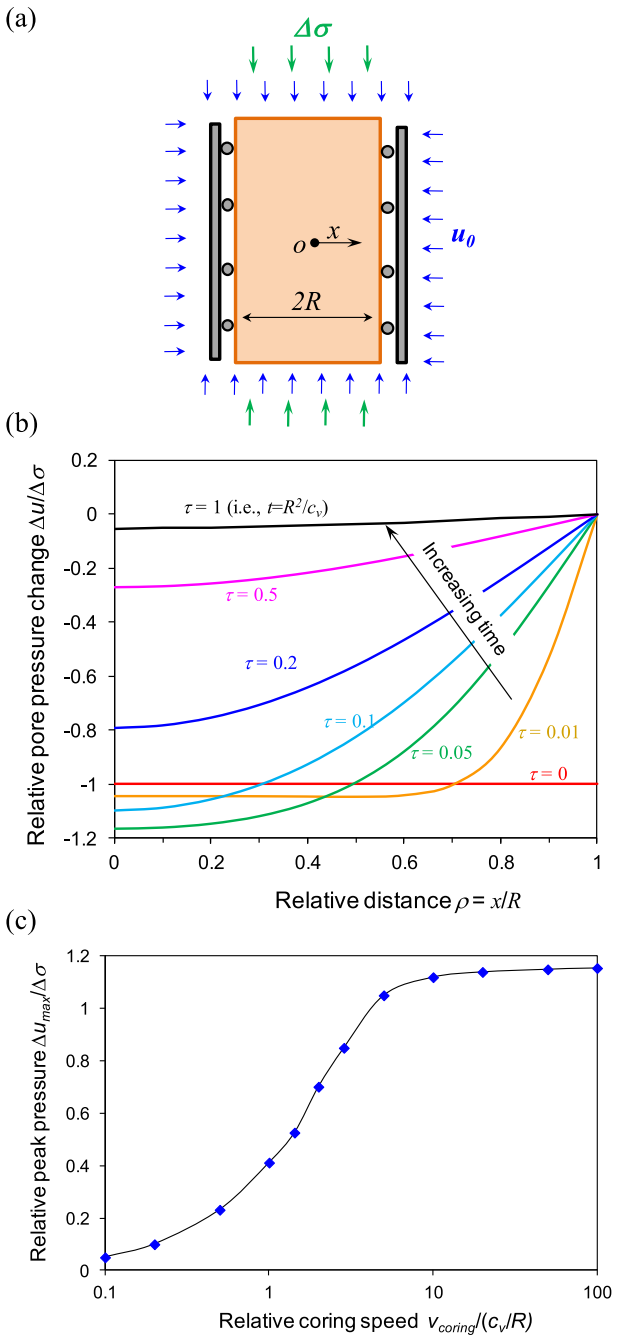


**Figure 5.** Vertical stress relaxation and pore pressure variation. (a) Poroelastic modeling: unloading $\Delta\sigma$ of a cylindrical specimen under zero-lateral strain conditions. Ambient water pressure is constantly $u_0$. (b) Unloading induced pore pressure distribution as a function of radial distance $\rho = x/R$ and time $\tau = tc_v/R^2$. (c) Peak pore pressure drop $\Delta u_{max}/\Delta\sigma$ as a function of the coring speed $v_{coring} = (c_v/R)$.

**Table 1**
Sediment parameters for the poroelastic model used to study the Mandel–Cryer effect in hydrate-bearing sediments.

| Properties | Unit | Value |
|---|---|---|
| Shear modulus, $G$ | MPa | 130 |
| Drained Poisson's ratio, $\nu$ | – | 0.2 |
| Undrained Poisson's ratio, $\nu_u$ | – | 0.46 |
| Porosity, $n$ | – | 0.4 |
| Skemption's coefficient, $B$ | – | 0.9 |
| Permeability, $k$ | mD | 0.1 |
| Fluid viscosity, $\mu$ | Pa·s | 0.001 |

Please cite this article in press as: Dai, S., Santamarina, J.C., Sampling disturbance in hydrate-bearing sediment pressure cores: NGHP-01 expedition, Krishna–Godavari Basin example, Marine and Petroleum Geology (2014), http://dx.doi.org/10.1016/j.marpetgeo.2014.07.013

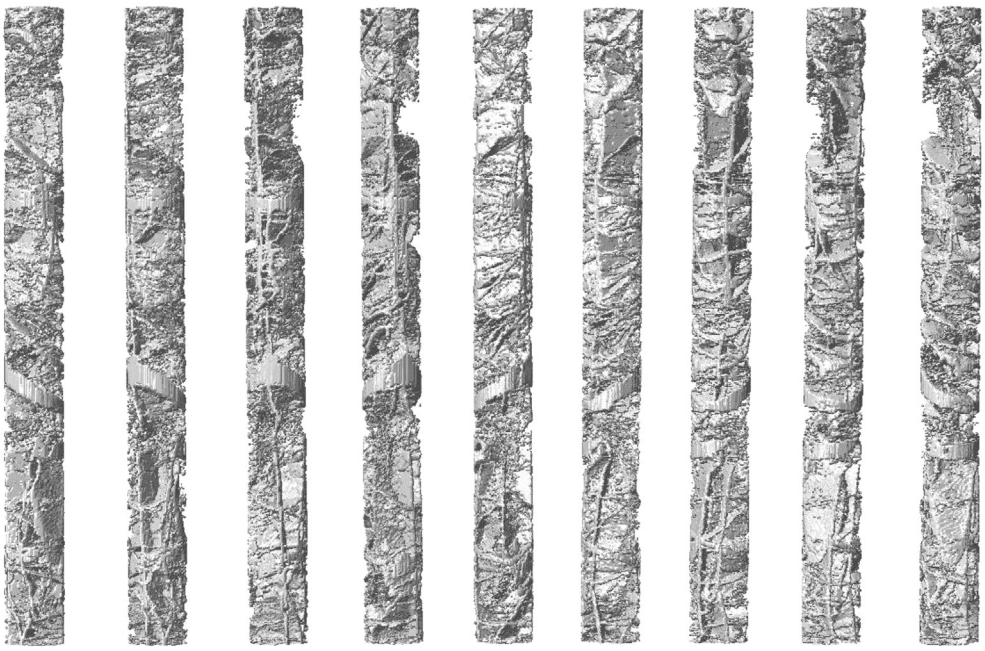

**Figure 6.** Is the long vertical hydrate lense along the core length a sampling induced hydrate artifact? Views of an X-ray tomograph captured every 20° (The tomogram gathered by Geotek was post processed to show the hydrate phase only). This hydrate-bearing sediment core was recovered from the Ulleung Basin; similar longitudinal lenses are observed in pressure cores recovered from the Krishna–Godavari Basin. The possibility of this long lense being a sampling artifact is most likely.

longitudinal features are observed in fine-grained sediments recovered from Krishna–Godavari Basin (Yun et al., 2010).

### 3.3. Post-sampling sediment creep and aging

The post-sampling stiffness evolution in frozen fine sands (Ottawa F110) with different ice saturations ($S_{ice} = 0.15$, 0.3, and 0.52) was experimentally examined in this study as an analog for hydrate-bearing sediments. The P-wave velocity of specimens after unloading (from 50 kPa to 1 kPa) decreases exponentially with time $V_{(t)}$:

$$V_{(t)} = V_0 - \Delta V\left(1 - e^{-\alpha t}\right) \tag{4}$$

where $V_0$ is the initial velocity, $\Delta V$ is the total velocity loss at infinite time, and $t_{ch} = 1/\alpha$ is the characteristic time for the stiffness creep. This relaxation time is $t_{ch} \approx 10$ min for all specimens in this study (Fig. 7). Such a short period suggests inevitable stiffness loss in hydrate-bearing sediments after sampling because most relaxation effects will have finished even before the core reaches the deck of the drill vessel.

Note that the compressive strength of methane hydrate is more than 20 times stronger than that of water ice under identical temperature and strain rate conditions (Durham et al., 2003), but their tensile and adhesive strength are similar (Jung and Santamarina, 2011). Therefore, the stiffness loss after unloading in hydrate-bearing sediments with cementation-type pore habit is expected to be comparable with results obtained with frozen soils shown here. While this pore habit is anticipated in excess gas systems only, it does provide an adequate upper bound for creep effects.

### 3.4. Core testing within the gas stability field conditions

Recovered hydrate-bearing sediments experience pressure and temperature changes, even when they are kept within the stability field using pressure core technology. Contrary to bulk conditions, methane solubility in water in the presence of methane hydrate increases with decreasing pressure and increasing temperature. The isochoric analysis of the variation in hydrate saturation due to pressure and temperature changes indicates that the decrease in methane solubility caused by a 1 K decrease in temperature is approximately equivalent to the effect induced by a 20 MPa pressure drop. In other words, a simultaneous decrease in both pressure and temperature with a gradient $\partial P/\partial T \approx 20$ MPa/K (dash line in Fig. 8) will not alter methane solubility or hydrate saturation. Thus, by neglecting the effects of pressure, the change in hydrate saturation $\Delta S_H$ can be estimated from the temperature change $\Delta T$ as (Appendix B):

$$\Delta S_H = 0.001\left(\frac{\Delta T}{1K}\right)\left(1 - S_{H_0}\right) \tag{5}$$

where $S_{H_0}$ is the initial hydrate saturation. Computed values show only minor changes in hydrate saturation with common laboratory pressure and temperature variations during pressure core testing. This observation allows testing hydrate-bearing sediments at lower and safer pressures without significant changes in the hydrate mass as long as minor changes in temperature are accounted for in the analysis. Gradual pressure-temperature changes will provide enough time to maintain equilibration conditions in the sediment core sample.

### 3.5. Anomalous hydrate preservation

Experiments show that methane hydrate can be temporarily preserved outside the stability field as local water temperatures fall below water freezing conditions; this is known as hydrate self-preservation or anomalous preservation (Stern et al., 2001; Yakushev and Istomin, 1992). This anomalous preservation regime extends from 240 K to 273 K at atmospheric pressure (Iwasaki et al., 2005; Melnikov et al., 2010; Stern et al., 2001). The lower bound of this regime 240 K is the transition temperature from cubic ice $I_c$ to hexagonal ice $I_h$, where the annealing of ice

Please cite this article in press as: Dai, S., Santamarina, J.C., Sampling disturbance in hydrate-bearing sediment pressure cores: NGHP-01 expedition, Krishna–Godavari Basin example, Marine and Petroleum Geology (2014), http://dx.doi.org/10.1016/j.marpetgeo.2014.07.013

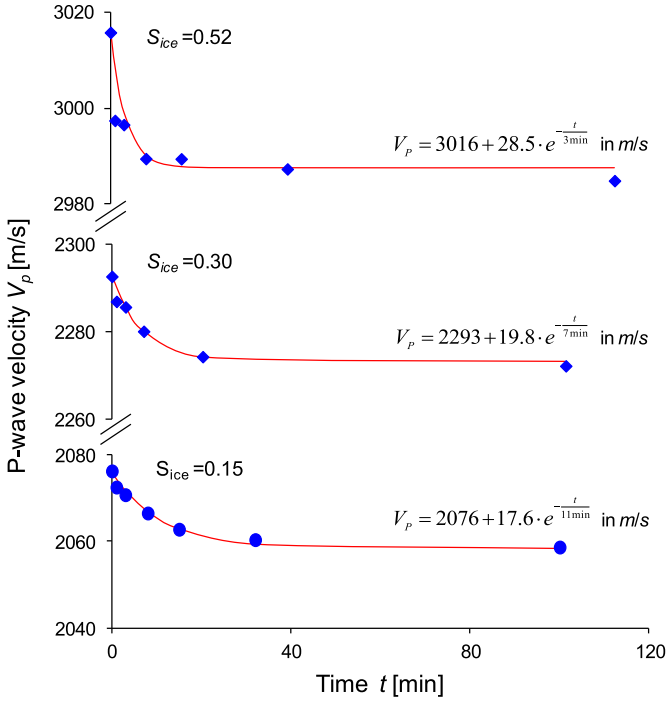


**Figure 7.** Stiffness creep after unloading (from 50 kPa to 1 kPa) for specimens with different ice saturations $S_{ice}$. Experimental data (markers) are fitted with an exponential decay model (lines).

stacking occurs (Kuhs et al., 2004; Murray and Bertram, 2006). Hydrate dissociation within this temperature regime undergoes four stages: (1) initial fast hydrate dissociation (Takeya et al., 2001); (2) supercooled water from hydrate dissociation forms a thin film of ice outside the residual hydrate crystals (Melnikov et al., 2009); (3) the ice shell slows down gas escape, yet it is not strong enough to encapsulate and fully stabilize the hydrate; and (4) hydrate dissociation virtually stops when the external ice shell is strong enough to keep inner hydrate stable; gradually, the included gas molecules within the encapsulated gas hydrate escapes by solid-state diffusion (Davidson et al., 1986; Stern et al., 2000; Takeya et al., 2001; Tse and Klug, 2002). The ice fraction that renders the maximum volume fraction of hydrate preserved by the ice shell is approximately 50%

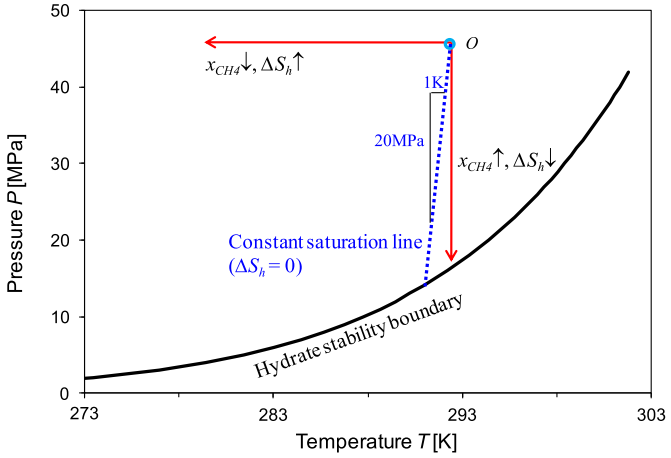


**Figure 8.** Effects of changes in pressure and temperature on hydrate saturation. The hydrate saturation within stability zone increases with decreasing temperature and increasing pressure. The change in hydrate saturation due to a 1 K decrease in temperature is approximately the same as produced by a 20 MPa increase in pressure.

at 240 K but less than 2% at 270 K, assuming the tensile strength of ice is $\sigma_t = 2.316 - 0.013(T/^\circ C)$ MPa (Petrovic, 2003).

Several other mechanisms are involved in self-preservation, including: (1) hydrate micro-structure in that quenched or rapidly cooled natural methane hydrate is noticeably less prone to fracturing or flaking than synthesized methane hydrate (Stern et al., 2001); (2) the time allowed to re-freeze the supercooled water ranges from tens of hours at 270 K to few seconds at 253 K, and it depends on the size of water droplets (Melnikov et al., 2009); (3) the ice cover formed at high degrees of supercooling will be less effective (Melnikov et al., 2010); and (4) Ostwald-ripening reduces grain to grain boundaries especially at higher temperatures.

The anomalous preservation of methane hydrate allows for the temporary manipulation and sub-sampling of frozen hydrate-bearing sediments without using high pressure chambers. Methane hydrate is also stable at $T < -80\ ^\circ C$ at atmospheric pressure. Therefore, hydrate-bearing sediments have been quenched in liquid nitrogen at atmospheric pressure to transfer core samples into test chambers when pressure core characterization technology is not available. But it is important to note that water freezing and expansion, and gas exsolution can cause irreversible core damage that may have marked effect on core properties such as the small-strain stiffness.

## 4. Discussion: characterization of hydrate-bearing sediments

### 4.1. Pressure core technology

Pressure core technology allows the manipulation (e.g., coring, transferring, sub-sampling, and testing) of hydrate-bearing sediments while maintaining pressure and temperature conditions within the hydrate stability field (Santamarina et al., 2012; Schultheiss et al., 2009).

Ideal sampling methods should maintain not only pressure and temperature, but also the effective stress throughout core manipulation and testing. Recompression tends to revert sampling disturbances except in brittle soft clays or loose sands (Bjerrum, 1973; Ladd and DeGroot, 2003; Landon, 2007). Restored effective stress is critical for the measurement of stress-dependent properties such as stiffness and strength in all sediments, including hydrate-bearing sediments.

### 4.2. Coring speed

Coring speed determines the unloading rate (i.e., stiffness loss) and affects the magnitude of transient pore pressure drop (i.e., possible dissociation and secondary hydrate formation). To minimize the transient pore pressure drop, the rate of coring $R/v_{coring}$ should be lower than the rate of pore pressure dissipation $R^2/c_v$, where $R$ is the specimen radius and $c_v$ is the pore water diffusion coefficient (see also Fig. 5c). Therefore, the coring velocity $v_{coring}$ for improved core quality should satisfy the following relationship:

$$v_{coring} << c_v/R. \tag{6}$$

Hydrate-bearing sediments in Krishna–Godavari Basin have $c_v \approx 1.2 \times 10^{-4}$ m$^2$/s (Yun et al., 2010). Consequently, the coring velocity should be significantly slower than $v_{coring} \leq 17$ m/h to allow pore pressure dissipation in a 5 cm-diameter core.

### 4.3. Coring system design

The following coring system characteristics may help reduce sample disturbance, based on the results of previous experimental

Please cite this article in press as: Dai, S., Santamarina, J.C., Sampling disturbance in hydrate-bearing sediment pressure cores: NGHP-01 expedition, Krishna–Godavari Basin example, Marine and Petroleum Geology (2014), http://dx.doi.org/10.1016/j.marpetgeo.2014.07.013

and numerical studies (Clayton and Siddique, 1999; Clayton et al., 1998; La Rochelle et al., 1980; Lunne et al., 2006):

- Sharp core shoe cutting angle: angle lower than 5°
- Thin sampler wall thickness: wall to radius ratio $t/R < 8\%$
- Low friction material along inside and outside corer walls
- Low inside clearance relative to the core radius $g/R$

The clearance between the liner and the sediment $g/R$ determines the core recovery ratio in soft unconsolidated sediments that swell against the liner during insertion. Consequently, there is a trade-off between preventing radial stress relaxation and plugging: smaller clearance $g/R$ minimizes specimen lateral strain, but leads to higher lateral stress on the inner wall and wall friction that may prevent the sediment from sliding into the sampler (i.e, jamming).

## 5. Conclusions

Sediment sampling causes unavoidable stress relaxation and strains that may alter the physical and mechanical properties of natural soils. Furthermore, pressure and temperature changes during sampling can cause additional disturbances to sediment samples when gas-rich fluids or hydrates are present within the core. The main lessons learned from field expeditions including the NGHP-01 Krishna–Godavari Basin expedition are:

- The prevailing hydrate topology in fine grained sediments consists of segregated hydrate in the form of nodules and lenses. Fine-grained sediments affect the hydrate stability zone and readily create undrained conditions (i.e., pore pressure change) during stress and strain variations, including sampling.
- Undrained unloading causes a marked transient pore pressure drop at the center of the specimen (i.e., poroelastic Mandel–Cryer effect). The coring speed should $v_{coring} << c_v/R$ to avoid undrained conditions.
- Pressure drop may couple with coring induced heating to trigger transient hydrate dissociation followed by secondary hydrate formation. The longitudinal hydrate lenses observed in tomographic images of pressure cores recovered from Krishna–Godavari Basin (India) and Ulleung Basin (Korea) may have been caused by poroelastic sampling effects.
- The expansion of the sediment skeleton during sampling may trigger hydrate tensile failure or hydrate-mineral debonding; these effects are lessened by slow coring/relaxation. The characteristic relaxation time is approximately 10 min for specimens analyzed in this study using ice as a hydrate analog. Such a short relaxation time suggests unavoidable stiffness loss in hydrate-bearing sediments after sampling because most relaxation effects will have asymptoted even before the core reaches the deck of the drill ship.
- The isochoric analysis of the variation in hydrate saturation due to $P$–$T$ changes shows that the decrease in methane solubility caused by a 1 K decrease in temperature is approximately offset by the change induced by a 20 MPa pressure drop. This observation allows testing hydrate-bearing sediments at lower and safer pressures without significant changes in the hydrate mass as long as minor changes in temperature are accommodated and changes are implemented at low rate to allow for equilibration.
- To minimize sampling disturbances, core samplers should have a sharp shoe cutting angle (<5°), thin sampler wall thickness ($t/R < 8\%$), low wall friction, and adequate inside clearance relative to the core radius $g/R$. There is a trade-off between preventing radial stress relaxation and core jamming: smaller clearance $g/R$ minimizes specimen lateral strain but leads to higher lateral stress on the inner wall and wall friction; thus, controlling the core recovery ratio in soft sediments.

## Acknowledgment

This research was supported by the Department of Energy/JIP project for methane hydrate, administered by Chevron. Additional funding is provided by the Goizueta Foundation.

## Appendix A. Supplementary data

Supplementary data related to this article can be found at http://dx.doi.org/10.1016/j.marpetgeo.2014.07.013.

## References

Atkinson, J.H., Allman, M.A., Boese, R.J., 1992. Influence of laboratory sample preparation procedures on the strength and stiffness of intact bothkennar soil recovered using the laval sampler. Geotechnique 42, 349–354.
Baligh, M.M., 1985. Strain path method. J. Geotech. Geoenviron. Eng. 111.
Baligh, M.M., Azzouz, A.S., Chin, C.T., 1987. Disturbances due to 'ideal' tube sampling. J. Geotech. Eng. 113, 739–757.
Banerjie, V., Mittal, A.K., Agarwal, K., Uniyal, A.K., Chandra, K., 1994. Carbon isotope geochemistry of petroleum-associated gases in Krishna–Godavari Basin, India. Org. Geochem. 21, 373–382.
Bastia, R., Nayak, P.K., 2006. Tectonostratigraphy and depositional patterns in Krishna offshore basin, Bay of Bengal. Lead. Edge 25, 839–845.
Basu, S., 1990. Clay mineralogy and pressure analysis from seismic information in Krishna–Godavari basin, India. Geophysics 55, 1447–1454.
Bjerrum, L., 1973. Problems of soil mechanics and construction of soft clays: state-of-the-Art report to session 4. In: 8th International Conference on Soil Mechanics and Foundation Engineering, Moscow, pp. 111–159.
Burland, J.B., 1990. On the compressibility and shear strength of natural clays. Géotechnique 40, 329–378.
Cao, P.-l., Yin, K., Peng, J.-m., Liu, J.-l., 2007. Optimization design and finite element analysis of core cutter. J. China Univ. Min. Technol. 17, 399–402.
Chau, K.W., 1991. Correlation of Sampling Effect in Hong Kong. A.A. Balkema, Bangkok, Thail, pp. 87–102.
Chung, S.G., Kwag, J.M., Giao, P.H., Baek, S.H., Prasad, K.N., 2004. A study of soil disturbance of pusan clays with reference to drilling, sampling and extruding. Geotechnique 54, 61–65.
Clayton, C.R.I., Siddique, A., 1999. Tube sampling disturbance-forgotten truths and new perspectives. Proc. Inst. Civ. Eng. Geotech. Eng. 137, 127–135.
Clayton, C.R.I., Siddique, A., Hopper, R.J., 1998. Effects of sampler design on tube sampling disturbance-numerical and analytical investigations. Geotechnique 48, 847–867.
Clennell, B.M., Hovland, M., Booth, J.S., Henry, P., Winters, W.J., 1999. Formation of natural gas hydrates in marine sediments 1. Conceptual model of gas hydrate growth conditioned by host sediment properties. J. Geophys. Res. 104, 22985–23003.
Collett, T., Riedel, M., Boswell, R., Cochran, J., Kumar, P., Sethi, A., Sathe, A., 2006. International Team Completes Landmark Gas Hydrate Expedition in the Offshore of India. In: Fire in the Ice, pp. 1–4.
Collett, T., Riedel, M., Cochran, J., Boswell, R., Kumar, P., Sathe, A., Party, T.N.E.S., 2008. Indian continental margin gas hydrate prospects: results of the Indian National Gas Hydrate Program (NGHP) Expedition 01. In: Proceedings of the 6th International Conference on Gas Hydrates (ICGH 2008), Vancouver, British Columbia, Canada.
Cryer, C.W., 1963. A comparison of the three dimensional consolidation theories of Biot and Terzaghi. Q. J. Mech. Appl. Math. 16, 401–412.
Dai, S., Lee, C., Carlos Santamarina, J., 2011. Formation history and physical properties of sediments from the Mount Elbert Gas hydrate stratigraphic test well, Alaska North Slope. Mar. Pet. Geol. 28, 427–438.
Dai, S., Santamarina, J.C., Waite, W.F., Kneafsey, T.J., 2012. Hydrate morphology: physical properties of sands with patchy hydrate saturation. J. Geophys. Res. Solid Earth 117.
Davidson, D.W., Garg, S.K., Gough, S.R., Handa, Y.P., Ratcliffe, C.I., Ripmeester, J.A., Tse, J.S., Lawson, W.F., 1986. Laboratory analysis of a naturally occurring gas hydrate from sediment of the Gulf of Mexico. Geochim. Cosmochim. Acta 50, 619–623.
Day, R.W., 1990. Sample disturbance of collapsible soil. J. Geotech. Eng. 116, 158–161.
Durham, W.B., Kirby, S.H., Stern, L.A., Zhang, W., 2003. The strength and rheology of methane clathrate hydrate. J. Geophys. Res. 108, 2182.
Eberhardt, E., Stead, D., Stimpson, B., 1999. Effects of sample disturbance on the stress-induced microfracturing characteristics of brittle rock. Can. Geotech. J. 36, 239–250.

Please cite this article in press as: Dai, S., Santamarina, J.C., Sampling disturbance in hydrate-bearing sediment pressure cores: NGHP-01 expedition, Krishna–Godavari Basin example, Marine and Petroleum Geology (2014), http://dx.doi.org/10.1016/j.marpetgeo.2014.07.013

Giao, P.H., Phien-Wej, N., Tanaka, H., 2004. An assessment on soil disturbance of Bangkok clay samples in relation with the intrinsic compression behavior. Lowl. Technol. Int. 6, 21–31.
Hemmingsen, B.B., Hemmingsen, E.A., 1980. Rupture of the cell envelope by induced intracellular gas phase expansion in gas vacuolate bacteria. J. Bacteriol. 143, 841–846.
Henry, P., Thomas, M., Clennell, M.B., 1999. Formation of natural gas hydrates in marine sediments: 2. Thermodynamic calculations of stability conditions in porous sediments. J. Geophys. Res. Solid Earth (1978–2012) 104, 23005–23022.
Hight, D.W., Boeese, R., Butcher, A.P., Clayton, C.R.I., Smith, P.R., 1992. Disturbance of the bothkennar clay prior to laboratory testing. Geotechnique 42, 199–217.
Hird, C.C., Hajj, A.R., 1995. Simulation of tube sampling effects on the stiffness of clays. Geotech. Test. J. 18, 3–14.
Hvorslev, M.J., 1949. Subsurface Exploration and Sampling of Soils for Civil Engineering Purposes. The Committee on Sampling and Testing, Soil Mechanics and Foundations Division, American Society of Civil Engineers, p. 521.
Iwasaki, H., Uchida, K., Nakamura, K., Suzuki, T., 2005. Continuous natural gas hydrate pellet production by process development unit. In: The Fifth International Conference on Gas Hydrates, Trondheim, Norway, pp. 1007–1015.
Jung, J.W., Jang, J., Santamarina, J.C., Tsouris, C., Phelps, T.J., Rawn, C.J., 2011. Gas production from hydrate-bearing sediments: the role of fine particles. Energy & Fuels 26 (1), 480–487.
Jung, J.W., Santamarina, J.C., 2011. Hydrate adhesive and tensile strengths. Geochem. Geophys. Geosyst. 12, Q08003.
Kimura, T., Saitoh, K., 1984. Effect of sampling disturbance on undrained strength of cohesive soils. Geotech. Eng. 15, 37–57.
Krishna, M.R., Chand, S., Subrahmanyam, C., 2000. Gravity anomalies, sediment loading and lithospheric flexure associated with the Krishna–Godavari basin, eastern continental margin of India. Earth Planet. Sci. Lett. 175, 223–232.
Kuhs, W.F., Genov, G., Staykova, D.K., Hansen, T., 2004. Ice perfection and onset of anomalous preservation of gas hydrates. Phys. Chem. Chem. Phys. 6, 4917–4920.
Kwon, T.-H., Cho, G.-C., Santamarina, J.C., 2008. Gas hydrate dissociation in sediments: pressure-temperature evolution. Geochem. Geophys. Geosyst. 9, Q03019.
La Rochelle, P., Sarrailh, J., Tavenas, F., Roy, M., Leroueil, S., 1980. Causes of sampling disturbance and design of design of a new sampler for sensitive soils. In: 33rd Canadian Geotechnical Conference: Problems and Progress in Geotechnical Engineering, Preprint Volume., Calgary, Alberta, Can, pp. 11. 12. 11-11. 12. 11.
Ladd, C.C., DeGroot, D.J., 2003. Recommended practice for soft ground site characterization: Arthur Casagrande Lecture. In: Proc. 12th Panamerican Conf. On Soil Mechanics and Geotechnical Engineering, MIT, pp. 3–57.
Landon, M.M., 2007. Development of a Non-destructive Sample Quality Assessment Method for Soft Clays. University of Massachusetts Amherst, United States – Massachusetts.
Landon, M.M., DeGroot, D.J., Sheahan, T.C., 2007. Nondestructive sample quality assessment of a soft clay using shear wave velocity. J. Geotech. Geoenviron. Eng. 133, 424–432.
Lee, J.Y., Santamarina, J.C., Ruppel, C., 2010. Volume change associated with formation and dissociation of hydrate in sediment. Geochem. Geophys. Geosyst 11, Q03007.
Lee, M.W., Collett, T.S., 2009. Gas hydrate saturations estimated from fractured reservoir at site NGHP-01-10, Krishna–Godavari Basin, India. J. Geophys. Res. Solid Earth 114, B07102.
Levadoux, J.-N., Baligh, M.M., 1980. Pore Pressures during Cone Penetration in Clays. Massachusetts Institute of Technology, Sea Grant College Program, Cambridge.
Li, X.S., Holland, J., Wang, G., Roblee, C.J., 1997. Analysis of stress-change disturbance caused by ideal drilling in clay. J. Geotech. Geoenviron. Eng. 123, 626–634.
Long, M., 2003. Sampling disturbance effects in soft laminated clays. Proc. Inst. Civ. Eng. Geotech. Eng. 156, 213–224.
Lunne, T., Berre, T., Andersen, K.H., Strandvik, S., Sjursen, M., 2006. Effects of sample disturbance and consolidation procedures on measured shear strength of soft marine Norwegian clays. Can. Geotech. J. 43, 726–750.
Mandel, J., 1953. Consolidation des sols. Geotechnique 3, 287–299.
Melnikov, V.P., Nesterov, A.N., Reshetnikov, A.M., Istomin, V.A., Kwon, V.G., 2010. Stability and growth of gas hydrates below the ice–hydrate–gas equilibrium line on the P–T phase diagram. Chem. Eng. Sci. 65, 906–914.
Melnikov, V.P., Nesterov, A.N., Reshetnikov, A.M., Zavodovsky, A.G., 2009. Evidence of liquid water formation during methane hydrates dissociation below the ice point. Chem. Eng. Sci. 64, 1160–1166.
Murray, B.J., Bertram, A.K., 2006. Formation and stability of cubic ice in water droplets. Phys. Chem. Chem. Phys. 8, 186–192.
Park, C.B., Clark, D.S., 2002. Rupture of the cell envelope by decompression of the deep-sea methanogen methanococcus jannaschii. Appl. Environ. Microbiol. 68, 1458–1463.
Petrovic, J.J., 2003. Review mechanical properties of ice and snow. J. Mater. Sci. 38, 1–6.
Rees, E.V.L., Priest, J.A., Clayton, C.R.I., 2011. The structure of methane gas hydrate bearing sediments from the Krishna–Godavari Basin as seen from Micro-CT scanning. Mar. Pet. Geol. 28, 1283–1293.
Rinaldi, V.A., Santamarina, J.C., 2008. Cemented Soils: Small Strain Stiffness, Deformational Characteristics of Geomaterials, Atlanta, GA, pp. 267–273.
Safaqah, O.A., Riemer, M.F., 2006. Minimizing sampling disturbance using a new in situ device. Soil. Dyn. Earthq. Eng. 26, 153–161.
Santagata, M., Germaine, J.T., 2005. Effect of OCR on sampling disturbance of cohesive soils and evaluation of laboratory reconsolidation procedures. Can. Geotech. J. 42, 459–474.
Santamarina, J., Jang, J., 2009. Gas production from Hydrate Bearing Sediments: Geomechanical Implications. In: NETL Methane Hydrate Newsletter: Fire in the Ice, vol. 9, pp. 18–22.
Santamarina, J.C., Dai, S., Jang, J., Terzariol, M., 2012. Pressure core characterization tools for hydrate-bearing sediments. Sci. Drill. 14, 44–48. http://dx.doi.org/10.2204/iodp.sd.2214.2206.2012.
Santamarina, J.C., Klein, A., Fam, M., 2001. Soils and Waves. John Wiley & Sons, New York.
Schultheiss, P.J., Holland, M., Humphrey, G., 2009. Wireline coring and analysis under pressure: recent use and future developments of the HYACINTH system. Sci. Drill. 7, 44–50.
Shankar, U., Riedel, M., 2011. Gas hydrate saturation in the Krishna–Godavari basin from P-wave velocity and electrical resistivity logs. Mar. Pet. Geol. 28, 1768–1778.
Shogaki, T., Kaneko, M., 1994. Effects of sample disturbance on strength and consolidation parameters of soft clay. Soils Found. 34, 1–10.
Siddique, A., Clayton, C.R.I., Hopper, R.J., 1999. The effects of varying centerline tube sampling disturbance on the behavior of reconstituted Clay. Geotech. Test. J. 22, 245–256.
Stern, L.A., Circone, S., Kirby, S.H., Durham, W.B., 2001. Anomalous preservation of pure methane hydrate at 1 atm. J. Phys. Chem. B 105, 1756–1762.
Stern, L.A., Kirby, S.H., Durham, W.B., Circone, S., Waite, W.F., 2000. Laboratory synthesis of pure methane hydrate suitable for measurement of physical properties and decomposition behavior. Coast. Syst. Cont. Margins 5, 323–348.
Stokoe, K.H., Santamarina, J.C., 2000. Seismic-wave-based testing in geotechnical engineering. Paper presented in International Society for Rock Mechanics – International Symposium, 19–24 November, Melbourne, Australia, pp. 1490–1536.
Takeya, S., Shimada, W., Kamata, Y., Ebinuma, T., Uchida, T., Nagao, J., Narita, H., 2001. In situ x-ray diffraction measurements of the self-preservation effect of CH4 hydrate. J. Phys. Chem. 105, 9756–9759.
Tanaka, H., Locat, J., Shibuya, S., Soon, T.T., Shiwakoti, D.R., 2001. Characterization of Singapore, Bangkok, and Ariake clays. Can. Geotech. J. 38, 378–400.
Tatsuoka, F., Shibuya, S., 1991. Deformation characteristics of soils and rocks from field and laboratory tests. In: Ninth Regional Conference on Soil Mechanics and Foundation Engineering. Organizing Committee for the Asian Regional Conference on Soil Mechanics and Foundation Engineering, Singapore, Bangkok, Thailand, pp. 101–170.
Tse, J.S., Klug, D.D., 2002. Formation and decomposition mechanisms for clathrate hydrates. J. Supramol. Chem. 2, 467–472.
Wallace, P.J., Dickens, G.R., Paul, C.K., Ussler III, W., 2000. Effects of core retrieval and degassing on the carbon isotope composition of methane in gas hydrate – and free gas-bearing sediments from the Blake Ridge. In: Paul, C.K., Matsumoto, R., Wallace, P.J., Dillon, W.P. (Eds.), Proceedings of the Ocean Drilling Program, Scientific Results. College Station, TX.
Yakushev, V.S., Istomin, V.A., 1992. Gas-hydrate self-preservation effect. In: Maeno, N., Hondoh, T. (Eds.), Physics and Chemistry of Ice. Hokkaido University Press, Sapporo, Japan, pp. 136–139.
Yun, T.S., Fratta, D., Santamarina, J.C., 2010. Hydrate-bearing sediments from the Krishna–Godavari Basin: physical characterization, pressure core testing, and scaled production monitoring. Energy & Fuels 24, 5972–5983.
Zhang, R., Lunne, T., 2002. Effect of sample disturbance on soft clay with low plasticity. Yanshilixue Yu Gongcheng Xuebao/Chinese J. Rock Mech. Eng. 21, 2350–2355.

Please cite this article in press as: Dai, S., Santamarina, J.C., Sampling disturbance in hydrate-bearing sediment pressure cores: NGHP-01 expedition, Krishna–Godavari Basin example, Marine and Petroleum Geology (2014), http://dx.doi.org/10.1016/j.marpetgeo.2014.07.013